Author's personal copy

Atmospheric Environment 50 (2012) 349–359

Contents lists available at SciVerse ScienceDirect

Atmospheric Environment

journal homepage: www.elsevier.com/locate/atmosenv

The chemical composition of surface snow in the Arctic: Examining marine, terrestrial, and atmospheric influences

Laura Krnavek [a,b,1], William R. Simpson [a,b,*], Daniel Carlson [a,b], Florent Domine [c,d], Thomas A. Douglas [e], Matthew Sturm [e]

[a] Department of Chemistry and Biochemistry, University of Alaska Fairbanks, Fairbanks, AK 99775-6160, USA
[b] Department of Geophysical Institute, University of Alaska Fairbanks, Fairbanks, AK 99775-6160, USA
[c] TAKUVIK Joint International Laboratory, Université Laval, 1045, ave. de la Médecine, Québec, QC G1V 0A6, Canada
[d] Centre national de la Recherche Scientifique, 3, rue Michel-Ange 75794 Paris Cedex 16, France
[e] US Army Cold Regions Research and Engineering Laboratory, Fort Wainwright, Alaska, USA

ARTICLE INFO

Article history:
Received 29 June 2011
Received in revised form
11 November 2011
Accepted 14 November 2011

Keywords:
Snow
Chemical composition
Ionic composition
Fractionation
Sea salt
Air–snow flux

ABSTRACT

We collected surface snow samples during three years (2004, 2005, and 2007) in Arctic Alaska and from the adjoining frozen Arctic Ocean during springtime in environments that span most Arctic terrains including land, thin and thick first-year sea ice, and multi-year sea ice. The snow was analyzed for Br^-, Cl^-, SO_4^{2-}, NO_3^-, NH_4^+, Na^+, K^+, Mg^{2+} and Ca^{2+}. Source fractionation processes and atmospheric influences are important modification mechanisms that influence the ions. We find that Cl^-, K^+ and Mg^{2+} are primarily sourced by unfractionated sea salt and only show deviations from sea salt composition at low Na^+ concentrations. Bromide and Ca^{2+} are highly influenced by atmospheric processes that are evident at low sea salt tracer concentrations. Calcium enrichments are due to the addition of non-sea salt (nss) Ca^{2+} from dust and possibly other sources. Bromide enrichments are due to the addition of nss-Br^- and bromide depletions are due to bromine activation to the gas phase. Sulfate is affected by source fractionation at high Na^+ concentrations and by atmospheric addition at low Na^+ concentrations. Nitrate and NH_4^+ are not correlated with sea salt and show less concentration variability than sea salt ions. Modifications are related to time-integrated air–snow exchange fluxes for Br^-, SO_4^{2-} and Ca^{2+} and are in good agreement with observations of related gas-phase and aerosol species. This work reinforces our understanding of air–snow exchanges and their importance for atmospheric chemistry in the Arctic.

© 2011 Elsevier Ltd. All rights reserved.

1. Introduction

Snow is an important scavenger of pollutants, sea salt, acids and other chemical species worldwide, but particularly in the Arctic. Snow can store scavenged species and later liberate the accumulated species into the atmosphere through exchange or can provide species to terrestrial and marine ecosystems during snow melt runoff. An example of snow composition influencing Arctic atmosphere chemistry is halogen chemistry, which causes ozone destruction (Barrie et al., 1988; Bottenheim et al., 1990; Fan and Jacob, 1992; McConnell et al., 1992; Vogt et al., 1996; Tang and McConnell, 1996; Rankin and Wolff, 2002; Platt and Hönninger, 2003; Simpson et al., 2007a). The same halogens involved in ozone destruction are believed to participate in the oxidation of gaseous elemental mercury, which is then added to the ecosystem (Schröeder and Munthe, 1998; Lindberg et al., 2002; Khalizov et al., 2003; Wang and Pehkonen, 2004). Thus, a detailed understanding of the chemical composition of the snowpack is crucial for a better understanding of the Arctic atmosphere's composition and chemical reactions.

Two common sources of ions to the snow in Arctic Alaska and the surrounding frozen Arctic Ocean are sea salts and acid gases (Toom-Sauntry and Barrie, 2002; Dominé et al., 2004). Major sea salt ions include Na^+, Cl^-, SO_4^{2-}, Ca^{2+}, K^+, Mg^{2+}, Br^- and major ions from acid gases are H^+, Cl^-, Br^-, SO_4^{2-}, NH_4^+ and NO_3^-. The majority of studies that address the composition of the snowpack investigated interactions between snow and the atmosphere by tracking

* Corresponding author. Department of Chemistry and Biochemistry, 900 Yukon Drive, Room 186, UAF, Fairbanks, AK 99775-6160, USA. Tel.: +1 907 474 7235; fax: +1 907 474 5640.
E-mail addresses: Laura.Krnavek@erg.com (L. Krnavek), wrsimpson@alaska.edu (W.R. Simpson).
[1] Former name is Laura Alvarez-Avilés. Present address: Eastern Research Group, Measurement Division, 601 Keystone Park Drive, Suite 700, Morrisville, NC 27560, USA.

1352-2310/$ – see front matter © 2011 Elsevier Ltd. All rights reserved.
doi:10.1016/j.atmosenv.2011.11.033

Author's personal copy

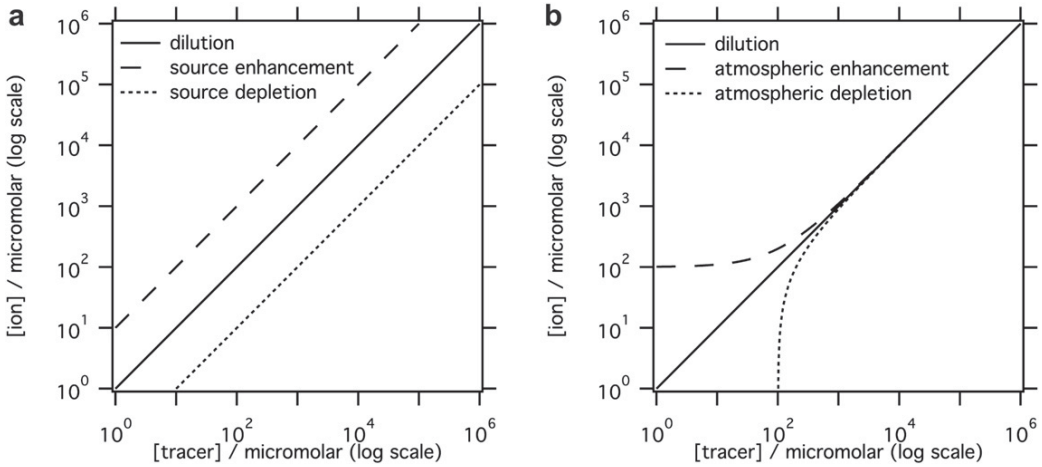

Fig. 1. A conceptual picture of modification patterns of ions in snow shown on log–log correlation plots. Panel a) shows the expected pattern if the source of ion into the snow was modified to be enriched (dashed line) or depleted (dotted line). Panel b) shows the enrichment (dashed line) and depletion due to exchange with the atmosphere.

modifications to chemical components in snow and the atmosphere (Joranger and Semb, 1989; Davidson et al., 1989; Udisti et al., 1999; Aristarain and Delmas, 2002; Gragnani et al., 2002; Toom-Sauntry and Barrie, 2002; Dominé and Shepson, 2002; Nikus, 2003; de Caritat et al., 2005; Benassai et al., 2005; Yalcin et al., 2006; Dibb et al., 2010). Enrichment factors, correlation coefficients, ternary plots and non-sea salt abundances are common tools to identify modifications in snow composition. However, the mentioned tools do not normally consider the sea salt tracer concentration range where modification occurs. In this paper we propose that correlation plots are an effective method to study the chemical composition of snow. Correlation plots consider the modifications to sea salt in context of the sea salt tracer concentration and can exhibit important details in enrichment or depletion patterns (Udisti et al., 1999; de Caritat et al., 2005; Simpson et al., 2005). These modification patterns may adopt shapes that could serve to identify specific processes that alter the chemical composition of snow, see section 2.

We classify the two most significant modification mechanisms that alter the ionic content of snow as source fractionation and atmospheric exchange. Source fractionation is a separation process in which ions separate before formation of aerosol or brine that is later incorporated into snow. An example of source fractionation is the precipitation of sea salts. These precipitation processes become thermodynamically favorable at certain temperatures. At −2 °C calcium carbonate precipitates ($CaCO_3$), possibly as calcite (Sander et al., 2006) but more likely as ikaite (Weeks and Ackely, 1982; Dieckmann et al., 2008; Morin et al., 2008), at −8 °C sulfate and sodium can precipitate as mirabilite ($Na_2SO_4 \cdot 10H_2O$) (Wagenbach et al., 1998; Rankin and Wolff, 2002), at −22 °C hydrohalite ($NaCl \cdot 2H_2O$) can crystallize (Rankin et al., 2000). When precipitation occurs, the precipitated crystal and residual solution may physically separate. Aerosol particles that form from the residual solution are now fractionated in the ion of interest (Rankin and Wolff, 2003; Alvarez-Avilés et al., 2008).

Atmospheric exchange describes the process of removing or adding ions via incorporation of aerosols and acids (addition) or heterogeneous reactions (removal). An example of atmospheric removal is halogen activation, which results in depleted Br^- in the snowpack (Simpson et al., 2005). Br^- is removed from the snowpack when it reacts with HOBr and yields photoactive bromine species (Fan and Jacob, 1992; McConnell et al., 1992; Vogt et al., 1996). The termination step of the gas-phase bromine chemistry occurs when bromine reacts with hydrocarbons to form HBr, which can add Br^- to surface snow. In addition to chemical reactions, acids stronger than HCl can displace Cl^- from aerosol particles or snow through reactions such as (Finlayson-Pitts, 2003)

$$2NaCl_{(aerosol)} + H_2SO_{4(aerosol)} \rightarrow 2HCl_{(gas)} + Na_2SO^{2-}_{4(aerosol)} \quad (R1)$$

$$NaCl_{(aerosol)} + HNO_{3(gas)} \rightarrow HCl_{(gas)} + NaNO_{3(aerosol)}. \quad (R2)$$

Removal of Cl^- as HCl would result in depletions (Yalcin et al., 2006), but snow or aerosols can scavenge HCl and add it to the sea salt Cl^- resulting in enrichments (Toom-Sauntry and Barrie, 2002; de Caritat et al., 2005; Benassai et al., 2005). A good acid candidate to remove Cl^- as HCl is sulfuric acid from Arctic haze, which can also add SO_4^{2-} to snow resulting in SO_4^{2-} enrichment (Li and Barrie, 1993).

2. Patterns caused by modification mechanisms

Fig. 1 shows two limiting cases of modification patterns to ions in snow shown as log–log correlation plots. Snow can vary approximately six orders of magnitude in Na^+ concentration from very pure inland snow ($[Na^+] \sim 1\ \mu M$) to cryo-concentrated sea salt brine ($[Na^+] \sim 1$ M), so we use log–log axes. Simple dilution of sea salt with condensed water vapor results in the solid diagonal lines in each panel of the plot. In Fig. 1a, we consider two source modifications, where sea salt is fractionated at its source either enriching (dashed line) or depleting (dotted line) the ion as compared to the sea salt tracer. Dilution subsequent to this source fractionation gives diagonal lines parallel to simple sea salt dilution. A common way to express source modification is through enrichment factors,

$$Ef[X] = \frac{\left(\frac{[X]}{[Na^+]}\right)_{Snow}}{\left(\frac{[X]}{[Na^+]}\right)_{Seawater.}} \quad (1)$$

Here, $[X]$ is the concentration of the ion of interest and $[Na^+]$ is the sodium concentration in snow or seawater. In Fig. 1a, the enriched line has $Ef = 10$, and the depleted line has $Ef = 0.1$. Thus, the

Author's personal copy

enrichment factor analysis is highly appropriate to describe source fractionation processes, particularly at high sea salt tracer concentrations.

Fig. 1b shows modification by exchange of ions with atmospheric aerosols or acids. Processes of this sort would be addition of atmospheric acidic gases or dust (e.g. sulfuric acid, Ca^{2+}), acid displacement (e.g. removal of Cl^- via addition of SO_4^{2-}), halogen activation (affects Br^-). Because this modification comes from or produces relatively limited fluxes between the snow and the atmosphere, we can model the fluxes as additions or removals of fixed concentrations of the ion of interest, with little or no correlation with sea salt abundance. The dashed line is the result when a fixed amount (100 μM) of the ion is added, and the dotted line corresponds when to fixed amount (100 μM) of the ion is removed. These lines curve because of the log–log plotting style. Atmospheric exchanges that result in enrichments and depletions are normally due to addition of non-sea salt (nss) ions to sea salt or removal of the ion from sea salt. To quantify the magnitude of ionic exchanges we can calculate the nss-ion (Equation (2)) from those samples that are affected the most by nss-ion additions,

$$\text{nss-}[X] = [X]_{\text{Sample}} - \left\{ \left(\frac{[X]}{[\text{Na}^+]} \right)_{\text{Seawater}} \times \left[\text{Na}^+ \right]_{\text{Sample}} \right\}. \quad (2)$$

The non-sea salt concentration for ion X is called nss-[X], $([X]/[Na^+])_{seawater}$ is the ion to Na^+ molar ratio in seawater, $[Na^+]_{sample}$ is the Na^+ concentration in the sample, and [X] is the ion concentration in the sample. Non-sea salt abundance analysis is appropriate to describe snow–atmospheric exchange; however, when the sea salt tracer concentration is high, the removal of sea salt background (the second term in equation (2)) becomes problematic due to the magnification of small errors in measurement of $[Na^+]$ and the ion of interest.

From Fig. 1, we can see these limited snow–air exchanges have little effect in the ion's behavior at high sea salt tracer contents but large effects at low tracer concentrations. Conversely, source fractionation affects the behavior at all tracer concentrations. Considering both panels together, we see that at low tracer concentrations atmospheric exchange is most evident while at high tracer concentrations source fractionation is most evident. Therefore, we see from these examples how log–log correlation plots allow separation of source fractionation from atmospheric exchange and provide more information than analyses of enrichment factors of non-sea salt abundance.

3. Methods

3.1. Sampling

The data set used in this paper is a compilation of three years of Arctic snow studies for a total of 936 surface snow samples, all obtained in Arctic Alaska and from the nearby frozen Arctic Ocean. Fig. 2 shows a map of the sampling locations. In 2004 a total of 104 surface snow samples were collected along a 102 km transect inland from Barrow, Alaska. In March and June 2005, 89 surface snow samples were collected on land-fast ice North of Point Barrow and additional samples were taken ~3 km inland from the coast, for a total of 122 samples. The samples from 2007 were collected from four different sites, both inland and on the sea ice. The two inland sites having 222 samples taken during March were located at 3 km and approximately 15 km from the shoreline in Barrow, Alaska. The two sea ice sites were in the Applied Physics Laboratory Ice Station (APLIS) ice camp, approximately 200 km north of Deadhorse, and on the land-fast ice near Barrow, Alaska. A total of 399 surface snow samples were collected on sea ice during the month of March and the first week of April. All of our samples were classified by one of four different environments: land, thin first-year sea ice (thin FYI), thick first-year sea ice (thick FYI) and multi-year sea ice (MYI). Thin FYI was a recently frozen lead (an opening in the sea ice), probably 2–3 weeks old and about 50 cm thick. Thick FYI was on the order of 170 cm thick and was likely formed in the preceding fall/winter. MYI is ice that has endured at least one summer melt season.

Samples were collected facing the wind wearing powder-free polyethylene disposable gloves and Tyvek suits. Sampling procedures outlined in Douglas and Sturm (2004) and Douglas et al. (2008) were used. All sampling vials were cleaned in the laboratory using 18.2 MΩ cm^{-1} water and were transported to the site packed in 1-gallon Ziploc bags. Snow was collected using the edge of the vial to scoop the top 2–3 cm of the surface snowpack. Snow stratigraphy and depth were measured at all sites, and snow depth was typical of windblown high Arctic (e.g. low total precipitation) conditions having depths 10–40 cm. All samples were transported and stored frozen and away from light until analysis.

3.2. Analytical procedures

The samples were melted and an aliquot was removed to measure specific conductivity (Oakton Instruments). Based on their conductivity, the samples were classified in groups for Ion

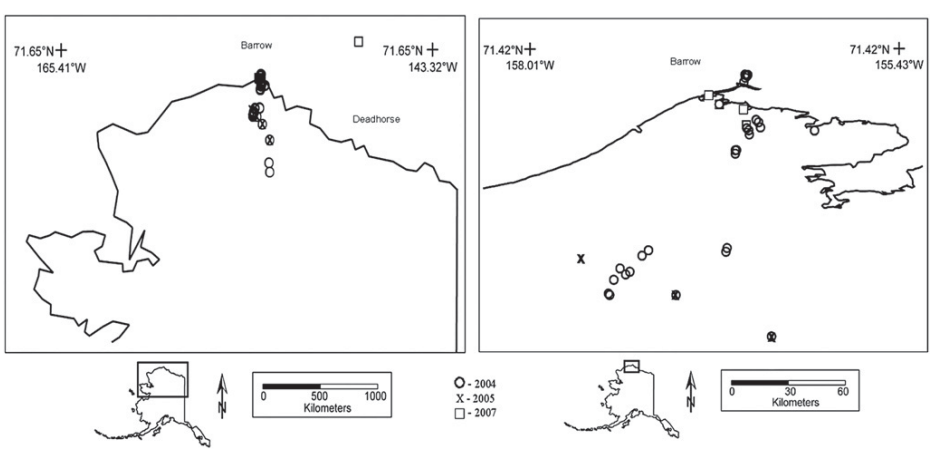

Fig. 2. A map of sampling locations in and near Arctic Alaska used in this study.

Author's personal copy

Chromatography (IC) analysis (DionexDX2000). Low concentration samples were analyzed without dilution, but higher concentration samples were diluted volumetrically such that the column was loaded near to but always below saturation of column sites. In this way, we maximized analytical precision while maintaining optimal peak shapes. To measure the instrument reproducibility, one sample was run 23 times for anions and 17 times for cations. The relative standard deviation for all ions in this analysis was less than 5%. To measure sampling variability we collected some snow in duplicates and calculated the ratio of the lower value divided by the higher value. The average for all ions was 0.85 indicating a 15% sampling variability, which is the same as reported by Dominé et al. (2004) who attributed the variability to wind deposition differences. Not all snow was collected in duplicate; 534 samples are single and 402 are duplicates. For snow that was collected in duplicates we report the average value.

Complex matrices like these snow samples contain other chemical species than the ones analyzed for this study. Our chromatographs show small peaks that according to their retention time could be organic acids (e.g. formate and acetate) that were not present in the standards and therefore were not quantified. The IC peak resolution for NH_4^+, Mg^{2+} and K^+ was relatively poor, causing increased noise associated with their measurement. For a short period of analysis, the cation suppressor malfunctioned, compromising the quantification of Mg^{2+} and K^+. Most samples were reanalyzed after instrumental repair, but a few had insufficient remaining sample volume, so the Na^+, Ca^{2+} and NH_4^+ data were used from the initial runs. Section 3.3 describes the method we used when various ions were missing in analysis. The ratio of ion to sea salt tracer was calculated from the standard seawater values reported by Quimby-Hunt and Turekian (1983).

3.3. Outlier identification

The ratio of the sum of cations to the sum of anions was used to identify outliers. Charge balance requires that the ratio of the sum of cations to the sum of anions be equal to one. When this ratio is not equal to one, anions or cations present in the snow were either not analyzed or analytical problems occurred. In our analysis, HCO_3^-/CO_3^{2-}, OH^-, organic acid anions, and H^+ are unanalyzed species. Fig. 3a shows the distribution of the charge balance ratio as a function of the number of observations of each ratio. When certain ion concentrations were missing, we added to the charge balance the expected contribution from sea salt of the missing ion. The histogram shows a high probability to measure a charge balance ratio of unity, as expected if the majority of ions are accounted for in the analysis. If we consider that the majority of the data appear to be in a normal (Gaussian) distribution, we expect that a range of the mean $\pm 6\sigma$ would encompass essentially all valid data. We consider data outside this range, mean $\pm 6\sigma$ (cation/anion ratio between 0.48 and 1.61), to be outliers that result from analytical error. A total of 65 of the 936 (7%) surface snow samples are considered outliers and are removed from the data set used in all subsequent analysis. Fig. 3b shows valid and outlier data. We recognize that samples with low values of anions and cations are more susceptible to atmospheric exchange. In order not to lose valuable information from samples at low sea salt tracer concentrations we keep all samples that contain less than 30 $\mu eq\ L^{-1}$.

4. Results

4.1. Charge balance and snow ionic content

Inspection of Fig. 3b indicates that the lower ionic strength samples tend to have more anion sum than cation sum, while as salinity increases the sums get closer to and may exceed the 1:1 line. To analyze this behavior, the log-averaged cation/anion ratio was calculated for three classes of ionic content. The least ionic samples, as defined by cation sum $<300\ \mu eq\ L^{-1}$ had an average cation/anion ratio of 0.76. The samples having intermediate ionic content (cation sum >300 and $<30{,}000\ \mu eq\ L^{-1}$) had an average cation/anion ratio = 0.94. The cation/anion ratio was 1.03 for the most ionic samples (cation sum $> 30{,}000\ \mu eq\ L^{-1}$). These results indicate the presence of acidity (excess unobserved protons) in the low salinity samples grading to alkalinity (excess unobserved HCO_3^-) for more saline samples. These observations are in agreement with the concept that atmospheric acid addition to snow will affect the least saline samples most and that seawater's alkalinity should be observed for high salinity samples.

Table 1 summarizes a statistical analysis of each ion's concentrations in all environments: land, multi-year sea ice (MYI), thick first-year sea ice (thick FYI), and thin first-year sea ice (thin FYI). To

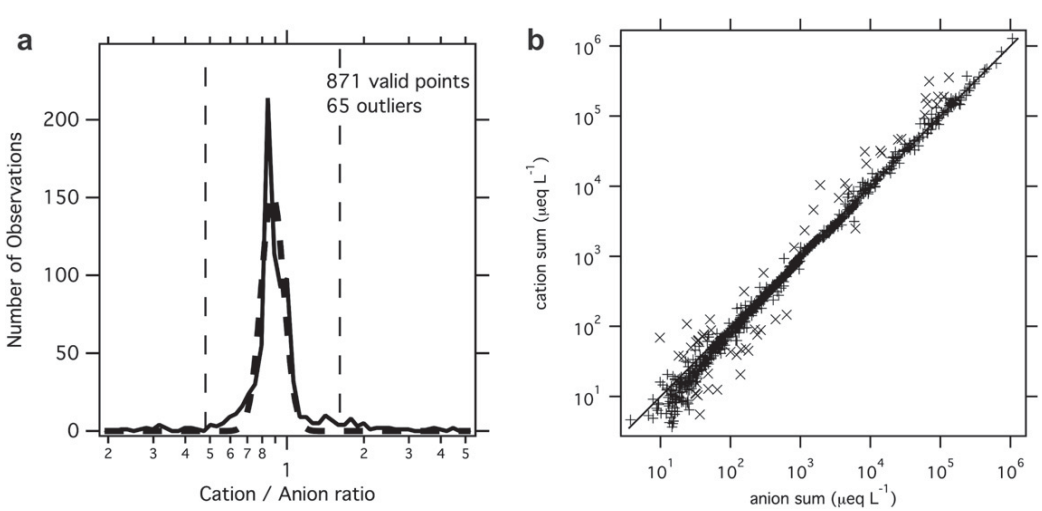

Fig. 3. Quality control analysis plots used to reject outlying data. Panel a) shows the distribution of the totality of 936 surface snow samples (solid line). The Gaussian curve (dashed) that best fits the data. Outliers are values outside the $+/-\ 6\sigma$ range. Panel b) shows the outliers as X symbols and valid data as plusses.

Author's personal copy

Table 1
Ranges and averages of each ion concentration (micromolar) in the four sampled environments.

Ion	Parameter	Land (μM)	MYI (μM)	Thick FYI (μM)	Thin FYI (μM)
Samples	Count	407	74	284	101
Na^+	Average	251.4	206.2	20,164	52,551
	Median	59.1	120.1	1569	9229
	10%	5.0	1.5	85	490
	90%	700.0	379.6	77,064	186,150
Cl^-	Average	353.3	305.6	21,058	63,217
	Median	106.7	175.5	2115	11,894
	10%	8.9	7.6	94	742
	90%	921.6	573.8	78,093	227,367
K^+	Average	6.5	5.1	318	834
	Median	2.8	3.3	24	95
	10%	0.1	0.1	1	6
	90%	15.3	11.1	1302	2345
Mg^{2+}	Average	34.8	30.7	1982	5169
	Median	13.0	19.6	146	574
	10%	0.6	0.3	6	33
	90%	91.1	64.2	8153	13,915
Ca^{2+}	Average	9.1	6.8	431	1032
	Median	4.6	5.2	29	112
	10%	1.2	1.2	2	10
	90%	21.3	12.9	1637	3074
Br^-	Average	0.26	0.32	30.6	92.5
	Median	0.15	0.25	2.0	17.9
	10%	0.04	0.06	0.2	1.2
	90%	0.56	0.40	108.7	317.3
SO_4^{2-}	Average	9.0	8.2	2044	1906
	Median	5.1	6.8	62	93
	10%	1.3	2.1	6	8
	90%	21.4	15.7	6426	6260
NO_3^-	Average	7.22	4.09	7.23	7.53
	Median	5.34	3.59	5.23	2.50
	10%	2.50	3.04	2.56	1.80
	90%	11.19	6.71	13.59	9.48
NH_4^+	Average	1.60	0.94	1.84	0.40
	Median	0.80	0.85	0.46	0.46
	10%	0.28	0.51	0.17	0.16
	90%	3.40	1.49	4.81	0.69

show a more representative range of concentrations we report here the 10th and 90th percentile. The 50th percentile is the median, and the average is calculated considering all values of the set.

The overall ionic content on land and on MYI appears to be similar and lower than concentrations on thin and thick FYI. The range of concentrations found on land is larger than on MYI, but the median values indicate that land samples have lower ionic contents than MYI samples. Thin FYI shows higher values in the range of concentrations, average and median than all other environments, therefore it has the highest overall ionic content. Ions that are generally low to absent in seawater (NO_3^- and NH_4^+) show small differences within their variability in the various environments.

4.2. Chloride (Cl^-) and sodium (Na^+)

Chloride (Cl^-) and sodium (Na^+) are the main constituents of seawater and can be used as sea salt tracers. Fig. 4a shows the correlation plot of Cl^- as a function of Na^+ in all environments. The majority of the data (80%) are within a factor of 2 of the seawater dilution line. The data above 1000 μM Na^+ is found in close proximity to the seawater dilution line. Considering the samples below 1000 μM Na^+, 86% of that subset are enriched in Cl^-, with an average enrichment factor of 1.33 for the enriched samples having less than 1000 μM Na^+. Reasons for the observed deviations and discussion of use of Cl^- as a sea salt tracer are presented in the discussion.

4.3. Potassium (K^+)

Fig. 4b shows the correlation plot for K^+. Potassium is correlated with sea salt with some scatter below 100 μM Na^+. The majority of the samples (85%) are found between the 2 times enriched and 2 times depleted lines. Of these samples that are between the 2 times enriched and 2 times depleted, half are enriched and half are depleted, indicating little net enrichment or depletion of K^+.

4.4. Magnesium (Mg^{2+})

Fig. 4c shows the Mg^{2+} correlation plot. Magnesium is correlated with sea salt with some scatter. The scatter may result from noise due to analytical errors or atmospheric exchange such as addition from dust. Similar to Cl^- and K^+, the majority of the samples (86%) are found between the 2 times enriched and 2 times depleted lines. However, unlike K^+, there appears to be a small net enrichment with 77% of all samples showing enrichment and 23% showing depletion. The enriched samples have an average enrichment factor of $Ef(Mg^{2+}) = 1.4$ while the depleted samples show an average enrichment factor of $Ef(Mg^{2+}) = 0.87$.

4.5. Calcium (Ca^{2+})

Fig. 4d is the correlation plot of Ca^{2+} with respect to Na^+. Calcium is correlated with sea salt at high Na^+ (above 100 μM) and shows enrichment at low Na^+ (below 100 μM). Almost all of the data below 100 μM Na^+ (91% of this subset) is found above the 2 times enriched line. In addition, a third of the samples below 100 μM are above the 10 times enriched line. At low Na^+ concentrations, the Ca^{2+} concentration becomes uncorrelated with sea salt and varies within a factor of ~5 of the 1 μM concentration. However, at high Na^+ concentration (above 100 μM), the Ca^{2+} data converges to the sea salt dilution line. The addition of Ca^{2+} in these data appears to be uncorrelated with sea salt, and is very similar to the atmospheric enrichment model of Fig. 1b.

4.6. Bromide (Br^-)

Fig. 5a shows the correlation plot of Br^- as a function of Na^+. Thin FYI is generally correlated with sea salt, while the other environments show atmospheric exchanges below 1000 μM Na^+ and correlate with sea salt above 1000 μM Na^+. The data below 1000 μM Na^+ represents 68% of the total data set and half of these samples enriched and half are depleted. Overall, these samples at less than 1000 μM Na^+ appear weakly correlated with sea salt and appear dominated by atmospheric exchanges. The Br^- concentration reaches an asymptote at low Na^+ concentration that is within a factor of 5 of 0.1 μM. Data at high Na^+ concentration converge to the sea salt dilution line.

4.7. Sulfate (SO_4^{2-})

Fig. 5b shows SO_4^{2-} versus Na^+ in all environments. In contrast to all other ions, SO_4^{2-} shows enrichments and depletions at high Na^+ concentrations, above 1000 μM, probably from source fractionation. Most samples above 1000 μM belong to thin and thick FYI. There appears to be a difference between thick and thin FYI, with thin FYI showing more depletion, while thicker FYI is more scattered across the sea salt dilution line. The majority of the thin FYI samples (84% of thin FYI samples with >1000 μM Na^+) are depleted as compared to 16% of the same subset that are enriched. In

Author's personal copy

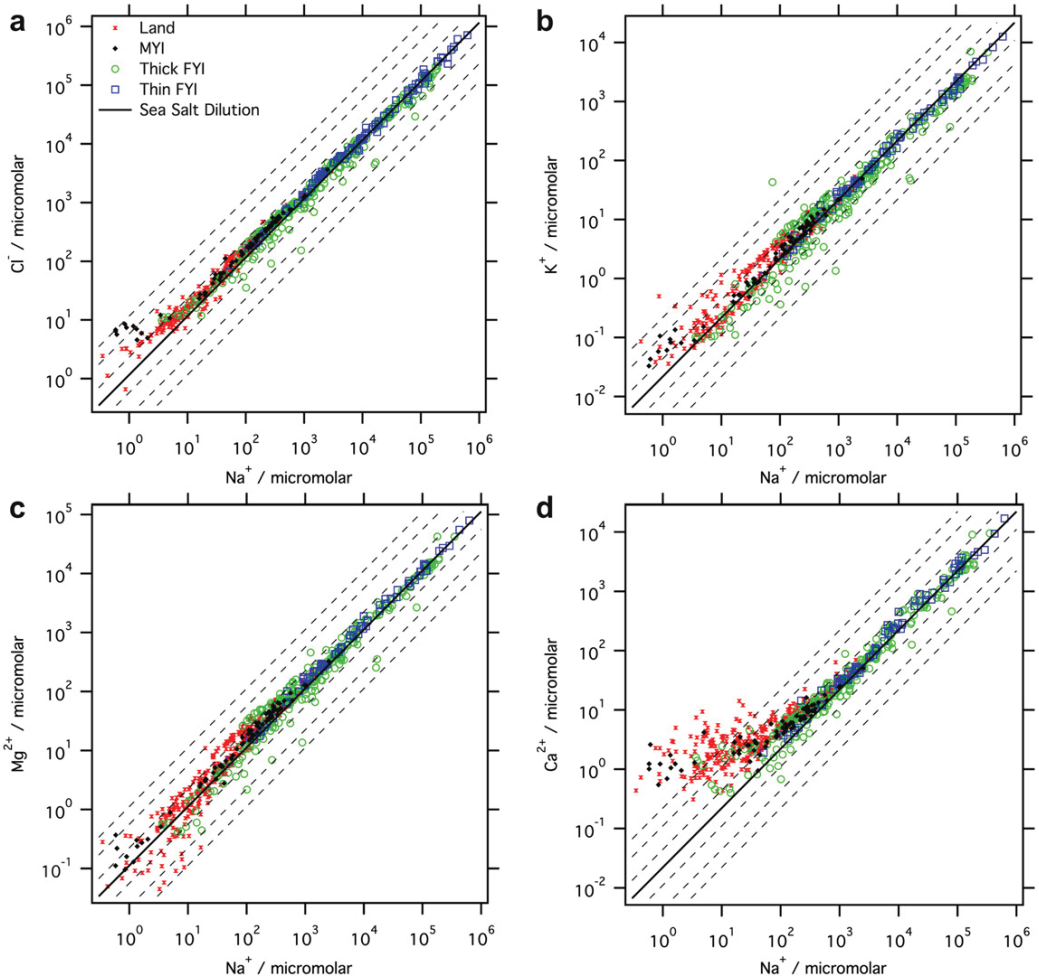

Fig. 4. Correlation plots of Cl^-, K^+, Mg^{2+}, and Ca^{2+} versus Na^+ in all four environments: land, thin-first-year sea ice (thin FYI), thick-first-year sea ice (thick FYI), and multi-year sea ice (MYI).The dashed lines above the seawater dilution line represent enriched snow with enrichment factors of 2, 5 and 10 times more than sea salt. The dashed lines below the seawater dilution line represents diluted snow with enrichment factors of 2, 5, and 10 times less than sea salt.

comparison, a thick FYI shows 60% of the samples having >1000 μM Na^+ are depleted as compared to 40% of the same subset that are enriched. Below 100 μM Na^+, SO_4^{2-} appears to reach an asymptote of approximately 1 μM.

4.8. Nitrate (NO_3^-) and ammonium (NH_4^+)

Table 1 and Fig. 5c and d show that NO_3^- and NH_4^+ are not correlated with sea salt. Because they are biologically utilized, the abundance of these two ions is variable and low in seawater; thus, the correlation plots do not show a seawater dilution line.

5. Discussion

5.1. Sodium and chloride as sea salt tracers

Sodium and Cl^- are good sea salt tracers and can be used to track modifications to sea salt (source fractionation and atmospheric exchange). Still, Na^+ and Cl^- are subject to modifications, and consideration of how these modifications affect the sea salt tracer helps to weigh the importance of these modifications. Chloride can be modified via acid displacement reactions, (R1) and (R2) (Finlayson-Pitts, 2003). The observed enrichment in Fig. 4a is due to the addition of hydrochloric acid to sea salt Cl^- in snow. The effect of HCl addition to snow diminishes as the sea salt tracer concentration increases. Below 1000 μM Na^+ most samples are within a factor of 2 from the sea salt concentration and they get closer to seawater concentration at higher Na^+ concentrations (above 1000 μM Na^+), indicating that Cl^- is generally a good sea salt tracer except for snow of very low marine influence.

Sodium can be modified via mirabilite precipitation, which removes SO_4^{2-} and Na^+, but because sea salt contains much more Na^+ than SO_4^{2-} (16.6:1, molar ratio), if all the available SO_4^{2-} is removed via mirabilite precipitation, only 12% of the sea salt Na^+ is lost (Rankin and Wolff, 2002), making it difficult to discern from the sea water dilution line in a log–log plot. Therefore, mirabilite precipitation is not a large modifier of Na^+, and Na^+ can be a good sea salt tracer for log–log plots. The same way depletion occurs via mirabilite precipitation, Na^+ enrichment could originate from addition of the precipitated mirabilite crystals to snow. However, these effects appear small and we can use either Na^+ or Cl^- as a good proxy for sea salt influence. We generally use Na^+ as the tracer, but have found that for anions, Cl^- is a lower noise tracer and as a consequence we use Cl^- in some interpretation plots.

Author's personal copy

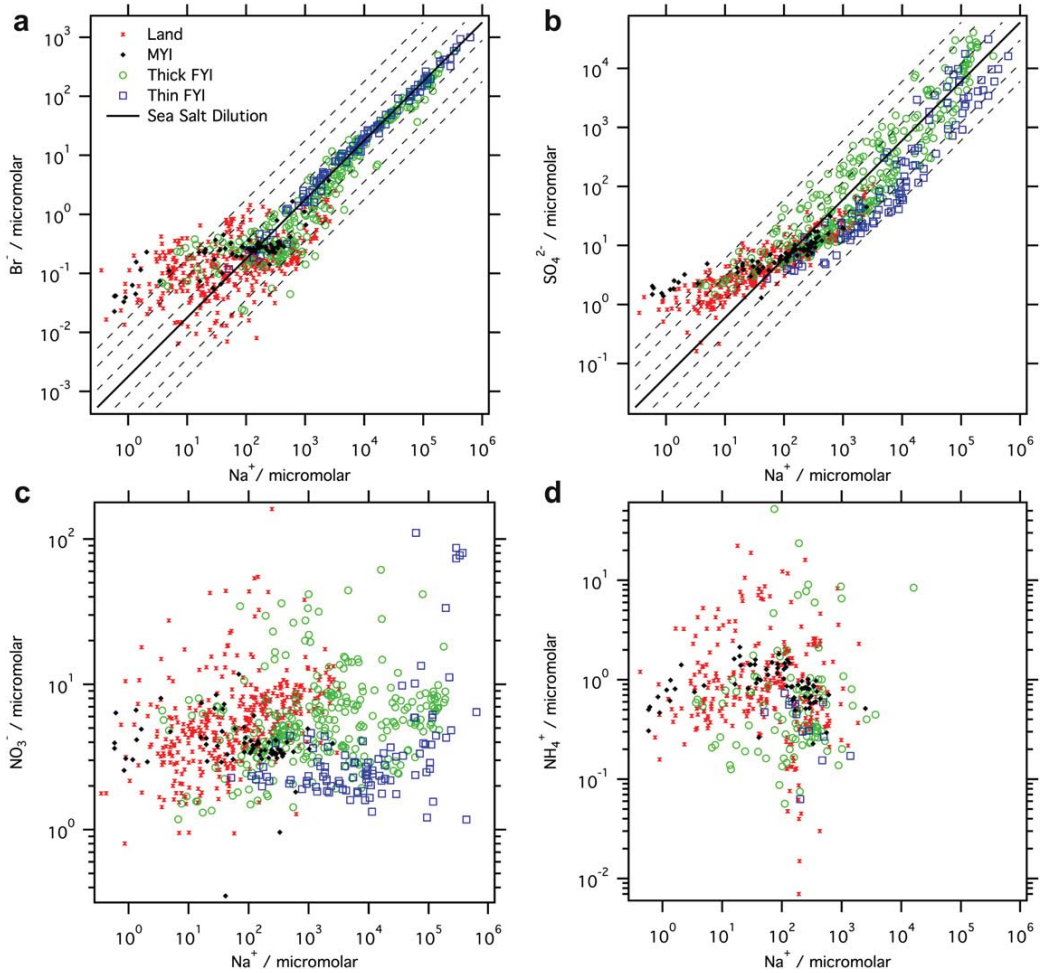

Fig. 5. Correlation plots of Br^-, SO_4^{2-}, NO_3^-, and NH_4^+ versus Na^+ concentrations. Ammonium was not quantified in most samples having Na^+ concentrations higher 1000 μM because the Na^+ peak overwhelmed the smaller NH_4^+ peak.

5.2. Ions correlated with seawater: potassium and magnesium

Magnesium and K^+ are correlated with seawater and show some values that we attribute to noise and possible addition from dust or removal via precipitation or substitutional incorporation in other precipitating minerals (e.g. mirabilite). The lack of net enrichment in the case of K^+ appears to indicate that noise or weak source fractionation is responsible for its variations. The small net enrichment of Mg^{2+} appears to argue for a small non-sea salt source like dust. However, this addition might be at least partially correlated with sea salt as evidenced by the lack of a plateau at the lowest Na^+ concentrations that is seen in Ca^{2+}, Br^-, and SO_4^{2-}. Source fractionation of Mg^{2+} and K^+ can occur through precipitation that becomes thermodynamically favorable at temperatures below −34 °C (Weeks and Ackely, 1982). However, the minerals precipitating from freezing sea water as described in Weeks and Ackely (1982) are pure stoichiometric phases while in reality solid solutions between minerals, ionic substitution within a mineral, or non-stoichiometry can greatly modify the actual composition of the precipitating phases. These processes have been extensively studied for major minerals of the Earth's crust (e.g. alkali feldspars – see Lagache and Carron, 1982). Sea salt minerals have been less studied, but substitution does take place. For example, Br^- substitutes for Cl^- in halite and sylvite (Siemann and Schramm, 2002). Sulfate minerals such as mirabilite also allow considerable ionic substitution because of their large crystal structures (Glynn, 2000). It is therefore likely that Mg^{2+} and K^+ can substitute for other ions in sea salt minerals, for example for Ca^{2+} in ikaite and for Na^+ in mirabilite, respectively, and show source fractionation.

5.3. An ion affected by atmospheric addition: calcium

Sea salt Ca^{2+} is the predominant Ca^{2+} source in snow samples with Na^+ concentrations above 100 μM and non-sea salt sources, possibly dust, dominate the total amount of Ca^{2+} in snow samples below 100 μM of Na^+. Calcium addition is significant at low Na^+ concentrations when a small addition carries more influence as compared to the same small addition to a highly concentrated sample. Dust sources normally contain both Ca^{2+} and Mg^{2+}, but the Mg^{2+} correlation plot is better correlated with sea salt at low Na^+ than the Ca^{2+} plot. One reason for this effect is that there is about 5 times more Mg^{2+} in seawater than Ca^{2+}, allowing enrichments in Ca^{2+} to be observed more easily over a lower sea salt "background" and that the amount of Ca^{2+} in mineral dust is usually larger than Mg^{2+}. The molar Ca^{2+}/Mg^{2+} ratio is between 2 and 10 for snow that

Author's personal copy

is not dominated by sea salt influences. Ice cores from Summit, have molar Ca^{2+}/Mg^{2+} ratios around 2 (Legrand and Mayewski, 1997). Snow from the French Alps, has a ratio of about 10 (Maupetit and Delmas, 1994), snow from Alert, is about 5 (Toom-Sauntry and Barrie, 2002), and snow studies at Longyearbyen, Svalbard, show a ratio of about 2 (Kang et al., 2001). Therefore, observations of Ca^{2+} enrichment by atmospheric deposition is due to the Mg^{2+}/Ca^{2+} ratio of sea salt being much larger than 1 and to the addition of atmospheric dust with Ca^{2+}/Mg^{2+} also much larger than 1 in many cases. It is also possible that Ca^{2+} is added from non-dust sources that apparently do not carry Mg^{2+}. Domine et al. (2011) proposed that exopolysaccharides (EPS) present in the surface microlayer of leads that open in sea ice could form Ca^{2+}-enriched aerosols. These EPS tend to form gel-like associations, cross-linked by divalent cations such as Ca^{2+} and excluding NaCl while retaining cell-related ions such as K^+ (Decho, 1990). Scavenging of these aerosols by snow or their deposition to snow could therefore contribute to the enrichment of snow in Ca^{2+} from the atmosphere. The enriched snow appears to reach an asymptotic Ca^{2+} concentration of around 1.7 μM. We obtained this value from the average of the nss-Ca^{2+} concentration (Equation (2)) in enriched snow at Na^+ concentrations below 100 μM. Fig. 6 contains a solid line that describes the overall pattern of Ca^{2+}.

5.4. An ion affected by atmospheric addition and removal: bromide

Snow can be a source and sink of Br^- via heterogeneous reactions that participate in halogen activation chemistry. As Br^- is removed from the snow (a source of atmospheric Br), the atmosphere transports the reactive bromine species (bromine atoms and BrO) farther from their removal site. This reactive bromine can react with aldehydes, HO_2, and VOCs to form HBr, which is ultimately returned to the snowpack, often elsewhere. The addition of HBr to snow with low sea salt Br^- concentration results in enrichments and the removal due to activation results in depletions. However, it is likely that the same snow has been subject to removal and addition of Br^- throughout time, which tends to cloud the overall picture of snow Br^- exchanges for low to moderate salinity snow. However, at the lowest sea salt tracer concentrations, we expect that atmospheric addition dominates over removal. We believe that the removal rate depends on snow concentration and the availability of Br^- to react and transform to reactive species, while the deposition rate should depend on the availability of a surface (surface snow, falling snow, particulates). We calculated the average of the minimum concentration range to be 0.2 μM using the nss-Br^- calculation (Equation (2)). In Fig. 7 the solid line shows the expected behavior when nss-Br^- is added to snow with low Br^- concentrations. Chloride was used instead of sodium because the bromide and chloride peaks are on the same chromatograph. The depleted samples below 1000 μM of Cl^- are found in the range of the minimum Br^- concentration and when considering nss-Br^- calculation result in negative values. Depletions below 1000 μM indicate that this snow served as a source of Br^- to the atmosphere and that the added HBr is not enough to result in positive nss-Br^- values. We estimated that the maximum removal of Br^- from snow that is observable on a log–log plot is 3 μM. The dotted line in Fig. 7 represents the removal of Br^-, and most of the samples lie between the enrichment and depletion models shown in this figure.

5.5. An ion affected by all modification mechanisms: sulfate

At low Cl^- concentrations, all snow samples show the same modification pattern for SO_4^{2-}, atmospheric addition (see Fig. 8). Arctic haze and other phenomena may be responsible for SO_4^{2-} addition into the snowpack as sulfuric acid (H_2SO_4) or ammonium sulfate ($(NH_4)_2SO_4$) (Shaw, 1995). The addition found at Cl^- concentrations less than 100 μM was calculated by averaging the nss-SO_4^{2-} concentration in all enriched samples less than 100 μM, resulting in an asymptotic concentration of around 1.7 μM.

At high Cl^- concentrations, SO_4^{2-} demonstrates source fractionation as shown in Fig. 8 by two approximately limiting models that are represented by dotted and solid lines. Limiting cases of enrichment and depletion appear to be roughly factors of 5 above and below the sea salt dilution line (Fig. 8). Sea salt SO_4^{2-} depletion occurs when Na^+ and SO_4^{2-} precipitate as mirabilite, which separates from the brine that contained sea salt SO_4^{2-} resulting in SO_4^{2-}-depleted brine. This SO_4^{2-}-depleted brine can be transported to surface snow by various processes including capillary rise

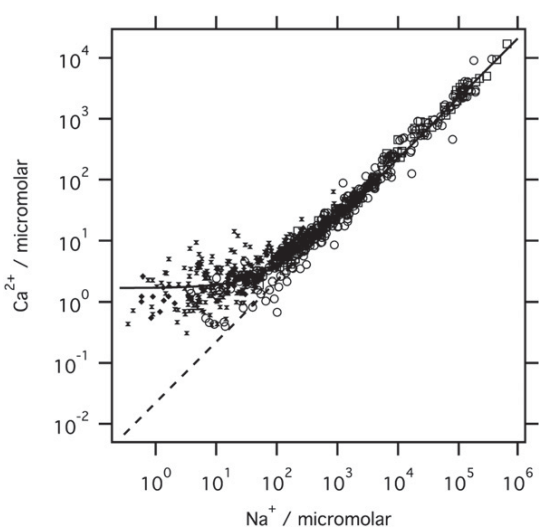

Fig. 6. Calcium modification model shown on a correlation plot of Ca^{2+} versus Na^+. The curvature at low Na^+ concentrations is the product of non-sea salt sources adding nss-Ca^{2+} to snow. As the sea salt tracer concentration increases, nss-Ca^{2+} influences are not significant and sea salt Ca^{2+} dominates the total amount of Ca^{2+}.

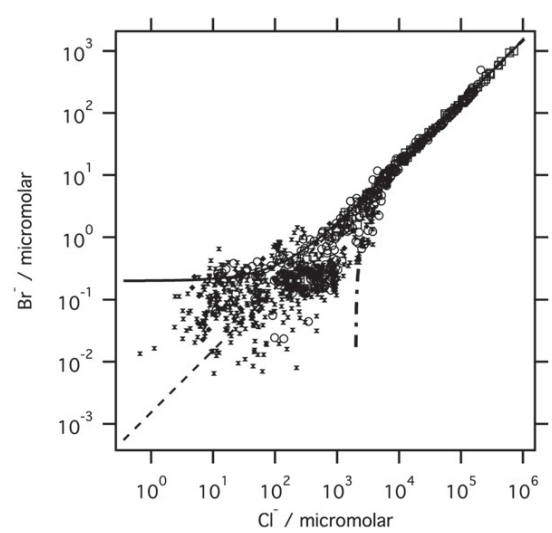

Fig. 7. Bromine modification models shown on a correlation plot of Br^- versus Cl^-. The Br^- atmospheric addition is shown in solid line and Br^- removal is shown as a dotted line.

Author's personal copy

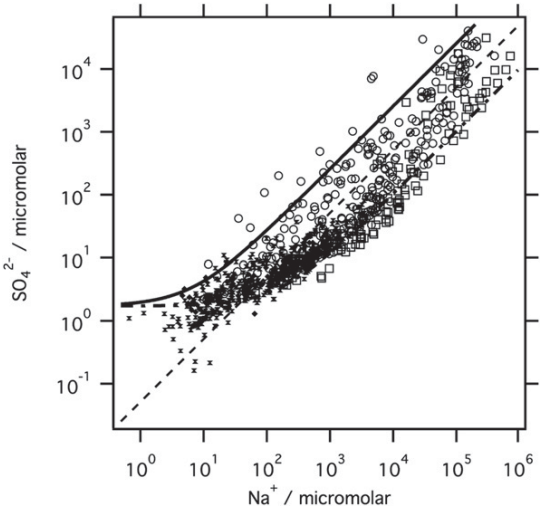

Fig. 8. Sulfate fractionation models shown on a correlation plot of SO_4^{2-} versus Na^+ Both dashed and solid lines are enriched at low sea salt tracer concentrations indicating addition from non-sea salt sources. The dashed line models source depletion, which appears more common in thin first year sea ice. The solid line represents source enrichment, which appears more common in thicker first-year sea ice.

(Coleou et al., 1999) or wind transport of snow contaminated by brine, and result in the observed SO_4^{2-} depletions in surface snow.

Thin FYI samples are more depleted in SO_4^{2-} than thick FYI samples. A possible explanation for this finding is that in young FYI, mirabilite precipitates and the brine that wicks up to surface snow is generally depleted in SO_4^{2-}. As the snow on FYI ages, wind may mix up snow layers and scour regions of the sea ice that have little snow cover. This mixing process could bring up mirabilite crystals to the surface of the snowpack, where they could enrich the surface snow samples in SO_4^{2-}. The fact that both MYI and land samples, which lack brine wicking as a possible ion transport mechanism, generally show depletions in their most concentrated Na^+ and Cl^- samples appears to indicate that aerosol arising from sea salts is generally depleted in SO_4^{2-}, as has been observed by Rankin and Wolff (2003).

5.6. Two ions uncorrelated with sea salt: nitrate (NO_3^-) and ammonium (NH_4^+)

Table 2 shows the ratio among NO_3^-, SO_4^{2-} and NH_4^+ in all of the studied environments. The ratio NH_4^+ to NO_3^- in all our samples, around 0.25. Nitrate and ammonium (NO_3^- and NH_4^+) are essentially absent in seawater and thus are not correlated with sea salt, although weak correlations may be present among various classes of samples (e.g. there appears to be a weak correlation of NO_3^- and Na^+ for land samples, for unknown reasons). The range of concentrations in NO_3^- and NH_4^+ show little variability (see Table 1). It appears that sources of NO_3^- and NH_4^+ in the snowpack are more constant than sea salt over the region that covers all sampled environments and that NO_3^- and NH_4^+ transport similarly to all the studied environments. Nitrate and ammonium also participate in biological transformations, which might occur in snowpack and smooth their distribution and reduce correlation with sea salt.

Because both NO_3^- and non-sea salt SO_4^{2-} are anthropogenic pollutants, one expects that they would be correlated, and previous aerosol and snow studies have found reasonable correlations between these two species (Toom-Sauntry and Barrie, 2002; Yalcin et al., 2006). However, the correlation we find in these data is as broad as the values reported by others indicating high variability and different transportation pathways for the sampled environments. For land snow, which is most comparable to the coastal/inland studies of Toom-Sauntry and Barrie (2002) and Yalcin et al. (2006), we find the NO_3^- to SO_4^{2-} ratio ranges from 0.3 to 3.5. This range is slightly different but overlaps that observed by Toom-Sauntry and Barrie (2002), who found a range of 0.2–0.6, and quite similar to Yalcin et al. (2006), who found a ratio of 1.09 that compares to our median of 1.05. The nitrate concentration is greater at Barrow than Alert probably because the snow collected in Barrow is aged in comparison to the referred Alert study, which analyzed freshly deposited snow. The increased sea salt at Barrow compared to Alert may also hold the pH more basic and allow more uptake of nitric acid via reaction R2. Nitrate snow chemistry, which has been extensively discussed in the literature (e.g. Honrath et al., 1999, 2000; Grannas et al., 2007), is also expected to be more dependent upon other ions in snow than sulfate because sulfuric acid and sulfur salts are not volatile, while nitric acid is semi volatile but nitrate salts are not. Thus aged particles may convert nitric acid

Table 2
Molar ratios among NH_4^+, NO_3^- and SO_4^{2-} for sampled environments and literature references. The compared references are samples of surface and/or fresh snow from costal sites and are most comparable to our land sample class. Analytical problems with detecting low ammonium amounts in the presence of high sodium probably biases the ratios of ammonium to other ions for highly saline samples (e.g. thin and thick FYI classes).

Ratio	Parameter	Land	MYI	Thin FYI	Thick FYI	Reference value
NH_4^+/NO_3^-	Count	282	72	99	13	
	Average	0.26	0.25	0.32	0.16	
	Median	0.15	0.24	0.11	0.15	
	10%	0.04	0.13	0.04	0.06	
	90%	0.51	0.42	0.28	0.31	
	Yalcin et al. (2006)	–	–	–	–	0.735
NO_3^-/SO_4^{2-}	Count	411	74	281	101	
	Average	1.62	0.87	0.27	0.10	
	Median	1.05	0.53	0.10	0.027	
	10%	0.41	0.24	0.0014	0.0012	
	90%	3.53	2.19	0.62	0.34	
	Yalcin et al. (2006)	–	–	–	–	1.09
	Toom-Sauntry and Barrie (2002)	–	–	–	–	0.2–0.6
NH_4^+/SO_4^{2-}	Count	282	72	99	13	
	Average	0.52	0.19	0.12	0.08	
	Median	0.21	0.18	0.04	0.07	
	10%	0.03	0.05	0.01	0.02	
	90%	0.98	0.38	0.27	0.18	
	Yalcin et al. (2006)	–	–	–	–	0.943

Author's personal copy

to salt forms (e.g. $NaNO_3$) that are less volatile and retained in the snow. Overall, the case of nitrate is complex, with sources that are not simply related to sea salt aerosols and chemical loss and probable recycling into the snowpack. Therefore, the lack of correlation of nitrate with sea salt tracers found in this study is probably expected. A more detailed analysis or future study that also considers likely time history of snow samples and changes in photochemical conditions is clearly needed.

5.7. Ionic abundances in snow in relation to atmospheric abundance

The abundance of certain ions in snow can be compared to the atmospheric abundance of related compounds to provide information on the role of snow as a source or sink of species in the atmosphere. The snow sampled here has gone through series of removal and addition steps of pollutants over time, reflecting a range of snow–atmosphere exchange extent. For conversion between snow concentration modifications and atmospheric abundance (atmospheric concentration) we consider the coupled part of the atmosphere to be a well-mixed column of 1 km height and the portion of the snowpack undergoing exchange to be 3 cm deep and have a density of 0.33 g cm^{-3} (Dominé et al., 2004; Douglas and Sturm, 2004). The water-equivalent height of the exchanging snowpack is 1 cm under the conditions above and we assume the air molecular density to be 3×10^{19} molecules cm^{-3}. Considering that the atmosphere and snowpack height can change by an order of magnitude, each of these estimates is expected to be accurate to an order of magnitude.

Calcium exhibits atmospheric addition that we interpret to be from crustal or possibly biological sources. From the correlation plot of Ca^{2+} (Fig. 6) we approximated the influence of these crustal sources to add an average of 1.7 μM of Ca^{2+} to snow. Using the assumptions discussed above, we calculate the equivalent atmospheric abundance of aerosol-particle-bound Ca^{2+} to be 0.7 μg m^{-3}, where that concentration from the 1 km atmospheric abundance would be added to the underlying snow column. Alternatively, one could get the same addition to snow by a lower atmospheric abundance depositing to the snowpack over a longer period of time. Observed aerosol particle Ca^{2+} concentrations at Alert are ~0.046 μg m^{-3} (Kawamura et al., 2007) and at NyÅlesund are ~0.032 μg m^{-3} (Teinilä et al., 2003). If one were to assume that the snowpack was aged enough to have received the aerosol particle calcium from roughly 10 to 20 atmospheric columns before the sampling time, the aerosol abundance at Alert or NyÅlesund could explain the amount of calcium ions added to snow. The difference between observations of aerosol and snow Ca^{2+} concentrations could be because different sources of dust bring Ca^{2+} to different parts of the Arctic. Many of our Ca^{2+}-enriched samples are from inland areas in Alaska near the Brooks mountain range, while Alert lies at higher latitudes in the Arctic and NyÅlesund experiences more marine conditions due to persistent nearby open water.

Interpretation of the Br^- correlation plot, Fig. 7, provided an approximation of the maximum atmospheric removal of Br^- from the snow to be 3 μM (section 5.4) and of maximum addition of Br^- to be 0.2 μM. Again, using the above assumptions, we obtain a maximum addition of 40 pptv atmospheric bromine (as Br) added to the snowpack surface and a maximum removal of 600 pptv of atmospheric bromine leaving the snow. The addition of bromine to the snowpack is in reasonable agreement with observations of BrO that indicate peak levels around 50 pptv (Wagner et al., 2001; Höenninger and Platt, 2002). The maximal removal from snow is an order of magnitude larger than typical atmospheric abundances, which might indicate that some limited regions of relatively saline snow produce large amounts of reactive bromine that then spread over wider geographic regions. Many of these samples that show decreases in bromide concentration are from samples taken from the sea ice, particularly the more saline FYI, which is in agreement with the idea that snow on FYI is a source of reactive bromine (Simpson et al., 2007b). It is also possible that, if frost flowers produce large amounts of sea salt aerosol, this aerosol could release reactive bromine before depositing to the snowpack. This deposition of concentrated and Br^- depleted sea salt to snow would then appear in our samples as Br^- depleted snow.

Sulfate at low Na^+ concentrations shows atmospheric addition from sources other than sea salt. This SO_4^{2-} addition was approximated to be 1.4 μM from Fig. 7 in section 5.5. Using the same considerations as discussed above, the equivalent aerosol SO_4^{2-} concentration is 1.3 μg m^{-3}. This concentration is in agreement with observations of nss-SO_4^{2-} at Alert (1–2 μg m^{-3}) (AMAP, 1998), which is in agreement with the idea that Arctic Haze can add SO_4^{2-} from non-sea salt sources to the snowpack. However, the discussion of calcium above indicated that the deposition of calcium to snow might be integrated over time, as represented by multiple atmospheric columns accumulating in the snow over time. Possibly particle size differences might cause a difference in the depositional behavior of sodium and calcium ions to the snowpack. At high Na^+ concentrations there are SO_4^{2-} enrichments and depletions that are not explained by atmospheric fluxes, and thus we interpret them as source fractionation of SO_4^{2-} through mirabilite precipitation and sea ice formation processes as explained in section 5.5.

6. Conclusions

Correlation plots of major ions in snow with respect to sea salt tracers show unique modification patterns for each ion. The modification pattern's shape depends on how the ion is affected by source fractionation and atmospheric exchange. Potassium and Mg^{2+} are comparable to the values observed in sea salt, and Ca^{2+} is observably enhanced by dust or other sources. Atmospheric aerosol Ca^{2+} concentrations appear to be in reasonable agreement with snow enhancements. Bromide is affected by atmospheric exchanges that both remove and add Br^- through atmospheric bromine chemistry. Maximum depletion of bromine from snow is roughly an order of magnitude larger than maximum enhancement, indicating that bromine may be sourced from limited geographic regions, and the resulting atmospheric bromine is deposited over wider geographic regions. Sulfate modifications suggested that SO_4^{2-}-depleted brine is the main source of SO_4^{2-} for surface snow and that SO_4^{2-}-enriched brine is unique to first-year sea ice. Addition of non-sea salt SO_4^{2-} at atmospheric aerosol abundances accounts for enrichment of SO_4^{2-} in surface snow that is observed at low sea salt tracer abundance. These observations provide valuable insight into the chemical composition of surface snow and snow–air interactions.

Acknowledgements

This work was funded by the National Science Foundation Office of Polar Programs Arctic Sciences Section: Sturm and Douglas (OPP-0435989) and Krnavek, Simpson, and Carlson (OPP-0435922 and ARC-0612457). Krnavek was supported by a US Department of Energy Global Change Education Program (GCEP) Graduate Research Educational Fellowship (GREF). Carlson was partially supported by a grant from the Cooperative Institute for Arctic Research (CIFAR). The Barrow Arctic Science Consortium (BASC) provided logistical support, and their assistance is greatly appreciated. We thank the University of Washington Applied Physics Laboratory Ice Station (APLIS) ice camp organizers for logistical support.

Author's personal copy

References

Alvarez-Avilés, L., Simpson, W.R., Douglas, T.A., Sturm, M., Perovich, D., Domine, F., 2008. Frost Flower chemical composition during growth and its implication for aerosol production and bromine activation. J. Geophys. Res. 113, D21304. doi:10.1029/2008JD010277.

AMAP, 1998. AMAP Assessment Report: Arctic Pollution Issues, Arctic Monitoring and Assessment Programme (AMAP), Oslo, Norway, IX, pp. 627–630.

Aristarain, A.J., Delmas, R.J., 2002. Snow chemistry measurements of James Ross Island (Antarctic Peninsula) showing sea salt aerosol modifications. Atmos. Environ. 36, 765–772.

Barrie, L.A., Bottenheim, J.W., Schnell, R.C., Crutzen, P.J., Rasmussen, R.A., 1988. Ozone destruction and photochemical reactions at polar sunrise in the lower Arctic atmophere. Nature 334, 138–141.

Benassai, S., Becagli, S., Graganani, R., Magand, O., Proposito, M., Fattori, I., Traversi, R., Udisti, R., 2005. Sea-spray deposition in Antarctic coastal and plateau areas from ITASE traverses. Ann. Glaciol. 41, 32.

Bottenheim, J.W., Barrie, L., Atlas, E., Heidt, L.E., Niki, H., Rasmussen, R.A., Shepson, P.B., 1990. Depletion of lower tropospheric ozone during Arctic spring: the Polar Sunrise Experiment 1988. J. Geophys. Res. 95 (D11), 18,555–18,568.

Coleou, C.C., Xu, K., Lesaffre, B., Brzoska, J.B., 1999. Capillary rise in snow. Hydrol. Process. 13 (12–13), 1721–1732.

Davidson, C.I., Harrington, J.R., Stephenson, M.J., Small, M.J., Boscoe, F.P., Gandley, R.E., 1989. Seasonal variations in sulfate, nitrate and chloride in the Greenland ice sheet: relation to atmospheric concentrations. Atmos. Environ. 23 (11), 2483–2493.

de Caritat, P., Hall, G., Gislason, S., Belsey, W., Braun, M., Goloubeva, N.I., Olsen, H.K., Scheie, J.O., Vaive, J.E., 2005. Chemical composition of arctic snow: concentration levels and regional distribution of major elements. Sci. Total Environ. 336, 183–199.

Decho, A.W., 1990. Microbial exopolymer secretions in ocean environments–their role (s) in food webs and marine processes. Oceanogr. Mar. Biol. 28, 73–153.

Dibb, J.E., Ziemba, L.D., Luxford, J., Beckman, P., 2010. Bromide and other ions in the snow, firn air, and atmospheric boundary layer at Summit during GSHOX. Atmos. Chem. Phys. 10, 9931–9942. doi:10.5194/acp-10-9931-2010.

Dieckmann, G.S., Nehrke, G., Papadimitriou, S., Göttlicher, J., Steininger, R., Kennedy, H., Wolf-Gladrow, D., Thomas, D.N., 2008. Calcium carbonate as ikaite crystals in Antarctic sea ice. Geophys. Res. Lett. 35, L08501. doi:10.1029/2008GL033540.

Dominé, F., Shepson, P.B., 2002. Air–Snow interactions and atmospheric chemistry. Science 297, 1506.

Dominé, F., Sparapani, R., Ianniello, A., Beine, H.J., 2004. The origin of sea salt in snow on Arctic sea ice and in coastal regions. Atmos. Chem. Phys. 4, 2259–2271.

Domine, F., Gallet, J.C., Barret, M., Houdier, S., Voisin, D., Douglas, T., Blum, J.D., Beine, H., Anastasio, C., 2011. The specific surface area and chemical composition of diamond dust near Barrow, Alaska. J. Geophys. Res. 116, D00R06, 18. doi:10.1029/2011JD016162.

Douglas, T.A., Sturm, M., 2004. Arctic haze, mercury and the chemical composition of snow across northwestern Alaska. Atmos. Environ. 38 (6), 805–820.

Douglas, T., Sturm, M., Simpson, W., Brooks, S., Lindberg, S., Perovich, D., 2008. Influence of snow and ice crystal formation and accumulation on mercury deposition to the Arctic. Environ. Sci. Technol. 42, 1542–1551.

Fan, S.M., Jacob, D.J., 1992. Surface ozone depletion in Arctic spring sustained by bromine reactions on aerosols. Nature 359, 522–524.

Finlayson-Pitts, B.J., 2003. The tropospheric chemistry of sea salt: a molecular-level view of the chemistry of NaCl and NaBr. Chem. Rev. 103, 4801.

Glynn, P., 2000. Solid-solution solubilities and thermodynamics: sulfates, carbonates and halides. Rev. Mineral. Geochem. 40, 481–511.

Gragnani, R., Smiraglia, C., Stenni, B., Torgini, S., 2002. Chemical and isotopic profiles from snow pits and shallow firn cores on Campbell Glacier, northern Victoria Land, Antarctica. Ann. Glaciol. X, 679.

Grannas, A.M., Jones, A.E., Dibb, J., Ammann, M., Anastasio, C., Ariya, P., Beine, H.J., Bergin, M., Bottenheim, J., Boxe, C.S., Carver, G., Chen, G., Crawford, J.H., Domine, F., Frey, M.M., Guzman, M.I., Heard, D.E., Helmig, D., Hoffmann, M.R., Honrath, R.E., Huey, L.G., Hutterli, M., Jacobi, H., Klan, P., McConnell, J., Sander, R., Savarino, J., Shepson, P.B., Simpson, W.R., Sodeau, J.R., von Glasow, R., Weller, R., Wolff, E., Zhu, T., 2007. An overview of snow photochemistry: evidence, mechanisms and impacts. Atmos. Chem. Phys. 7, 4329–4373.

Höenninger, G., Platt, U., 2002. Observations of BrO and its vertical distribution during surface ozone depletion at Alert. Atmos. Environ. 36, 2481–2490.

Honrath, R.E., Peterson, M.C., Guo, S., Dibb, J.E., Shepson, P.B., Campbell, B., 1999. Evidence of NOx production within or upon ice particles in the Greenland snowpack. Geophys. Res. Lett. 26, 695–698.

Honrath, R.E., Peterson, M.C., Dziobak, M.P., Dibb, J.E., Arsenault, M.A., Green, S.A., 2000. Release of NO_x from sunlight-irradiated midlatitude snow. Geophys. Res. Lett. 27, 2237–2240.

Joranger, E., Semb, A., 1989. Major ions and scavenging of sulphate in the Norwegian Arctic. Atmos. Environ. 23 (11), 2463–2469.

Kang, S., Qin, D., Mayewski, P., Gjessing, Y., 2001. Snow chemistry in Svalbard. Arctic. Bull. Glaciol. Res. 18, 9–13.

Kawamura, K., Narukawa, M., Ling, S.M., Barrie, L.A., 2007. Size distribution of dicarboxylic acids and inorganic ions in atmospheric aerosols collected during polar sunrise in the Canadian high Arctic. J. Geophys. Res. 112, D10307. doi:10.1029/2006JD008244.

Khalizov, A.F., Viswanathat, B., Larregaray, P., Ariya, P.A., 2003. A theoretical study on the reactions of Hg with halogens: atmospheric implications. J. Phys. Chem. 107, 6360–6365. doi:10.1021/jp0350722.

Lagache, M., Carron, J.P., 1982. Zonation of trace-elements in the course of the growth of crystals in silicate baths – the example of Rb, Cs, Sr, and Ba in the QZ-AB-OR-H2O system. Geochim. Cosmochim. Acta 46 (11), 2151–2158.

Legrand, M., Mayewski, P., 1997. Glaciochemistry of polar icecores: a review. Rev. Geophys. 35, 219–243.

Li, S.M., Barrie, L.A., 1993. Biogenic sulphur aerosol in the Arctic troposphere: I. Contributions to sulphate. J. Geophys. Res. 98D, 20613–20622.

Lindberg, S., Brooks, S., Lin, C.J., Scott, K.J., Landis, M.S., Stevens, R.K., Goodsite, M., Richter, A., 2002. Dynamic oxidation of gaseous mercury in the Arctic troposphere at Polar Sunrise. Environ. Sci. Technol. 36, 1245–1256.

Maupetit, F., Delmas, R., 1994. Snow chemistry of high altitude glaciers in the French Alps. Tellus 46 B, 304–324.

McConnell, J.C., Henderson, G.S., Barrie, L., Bottenheim, J., Niki, H., Langford, C.H., Templeton, E.M.J., 1992. Photochemical bromine production implicated in Arctic boundary-layer ozone depletion. Nature 355, 150–152.

Morin, S., Marion, G.M., von Glasow, R., Voisin, D., Bouchez, J., Savarino, J., 2008. Precipitation of salts in freezing seawater and ozone depletion events: a status report. Atmos. Chem. Phys. 8, 7317–7324. doi:10.5194/acp-8-7317-2008.

Nikus, U., 2003. Ion content of the snowpack on Franz Josef Land, Russia. Arctic Antarctic Alpine Res. 35 (3), 399–408.

Platt, U., Hönninger, G., 2003. The role of halogen species in the troposphere. Chemosphere 52, 325–338.

Quimby-Hunt, M.S., Turekian, K.K., 1983. Distribution of elements in Sea Water. Eos 64 (14), 130–132.

Rankin, A.M., Auld, V., Wolff, E.W., 2000. Frost flower as a source of fractionated sea salt aerosol in the polar regions. Geophys. Res. Lett. 27 (21), 3469–3472.

Rankin, A.M., Wolff, E.W., 2002. Frost flowers: implications for tropospheric chemistry and ice core interpretation. J. Geophys. Res. 107 (D23), 4683. doi:10.1029/2002JD002492.

Rankin, A.M., Wolff, E.W., 2003. A year-long record of size-segregated aerosol composition at Halley, Antartica. J. Geophys. Res. 108 (D24), 4775. doi:10.1029/2003JD003993.

Sander, R., Burrows, J., Kaleschke, L., 2006. Carbonate precipitation in brine – a potential trigger for tropospheric ozone depletion events. Atmos. Chem. Phys. 6, 4653–4658.

Schröeder, W.H., Munthe, J., 1998. Atmospheric mercury – an overview. Atmos. Environ. 32, 809–822.

Shaw, G.E., 1995. The Arctic haze phenomenon. Bull. Am. Meteorol. Soc. 76, 2403–2413.

Siemann, M.G., Schramm, M., 2002. Henry's and non-Henry's law behavior of Br in simple marine systems. Geochim. Cosmochim. Acta 66 (8), 1387–1399.

Simpson, W.R., Alvarez-Avilés, L., Douglas, T.A., Sturm, M., Dominé, F., 2005. Halogen in the coastal snowpack near Barrow Alaska: evidence for active bromine air–snow chemistry during springtime. Geophys. Res. Lett. 32 (L04811). doi:10.1029/2004GL021748.

Simpson, W.R., von Glasow, R., Riedel, K., Anderson, P., Ariya, P., Bottenheim, J., Burrows, J., Carpenter, L., Frieß, U., Goodsite, M.E., Heard, D., Hutterli, M., Jacobi, H.W., Kaleschke, L., Neff, B., Plane, J., Platt, U., Richter, A., Roscoe, H., Sander, R., Shepson, P., Sodeau, J., Steffen, A., Wagner, T., Wolff, E., 2007a. Halogens and their role in polar boundary-layer ozone depletion. Atmos. Chem. Phys. 7, 4375–4418.

Simpson, W.R., Carlson, D., Hoenninger, G., Douglas, T.A., Sturm, M., Perovich, D.K., Platt, U., 2007b. The dependence of Arctic tropospheric halogen chemistry on sea ice conditions. Atmos. Chem. Phys. 7, 621–627. doi:10.1029/2004GL022132.

Tang, T., McConnell, J.C., 1996. Autocatalytic release of bromine from Arctic snowpack during polar sunrise. Geophys. Res. Lett. 23, 2633–2636.

Teinilä, K., Hillamo, R., Kerminen, V.M., Beine, H.J., 2003. Aerosol chemistry during the NICE dark and light campaigns. Atmos. Environ. 37, 563–575.

Toom-Sauntry, D., Barrie, L.A., 2002. Chemical composition of snowfall in the high Arctic: 1990–1994. Atmos. Environ. 36, 2683–2693.

Udisti, R., Begagli, S., Castellano, E., Traversi, R., Vermigli, S., Piccardi, G., 1999. Sea-spray and marine biogenic seasonal contribution to snow composition at Terra Nova Bay, Antarctica. Ann. Glaciol. 29, 77.

Vogt, R., Crutzen, P.J., Sander, R., 1996. A mechanism for halogen release from sea salt aerosol in the romote marine boundary layer. Nature 338, 327–330.

Wagenbach, D.F., Ducroz, R., Mulvaney, L., Keck, A., Minikin, M., Legrand, J.S.Hall, Wolff, E.W., 1998. Sea salt aerosol in coastal Antarctic regions. J. Geophys. Res. 103 (D9), 10,961–10,974.

Wagner, T., Leue, C., Wenig, M., Pfeilstcker, K., Platt, U., 2001. Spatial and temporal distribution of enriched boundary layer BrO concentrations measured by the GOME instrument aboard ERS-2. J. Geophys. Res. 106 (D20), 24,225–24,235.

Wang, Z., Pehkonen, S.O., 2004. Oxidation of elemental mercury by aqueous bromine: atmospheric implications. Atmos. Environ. 38, 3675–3688.

Weeks, W.F., Ackely, S.F., 1982. The growth structure and properties of sea ice, Open File Rep. Monogr., 82-1, 130 pp., CRREL, USA.

Yalcin, K., Wake, C.P., Dibb, J.E., Whitlow, S.I., 2006. Relations between aerosol and snow chemistry at King Col, Mt. Logan Massif, Yukon Canada. Atmos. Environ. 40, 7152–7163.